arXiv:1011.4107v1 [astro-ph.CO] 17 Nov 2010

STELLAR STRUCTURE AND TESTS OF MODIFIED GRAVITY

Philip Chang[1] & Lam Hui[2]
Draft version November 19, 2010

ABSTRACT

Theories that attempt to explain cosmic acceleration by modifying gravity typically introduces a long-range scalar force that needs to be screened on small scales. One common screening mechanism is the chameleon, where the scalar force is screened in environments with a sufficiently deep gravitational potential, but acts unimpeded in regions with a shallow gravitational potential. This leads to a variation in the overall gravitational G with environment. We show such a variation can occur within a star itself, significantly affecting its evolution and structure, provided that the host galaxy is unscreened. The effect is most pronounced for red giants, which would be smaller by a factor of tens of percent and thus hotter by 100's of K, depending on the parameters of the underlying scalar-tensor theory. Careful measurements of these stars in suitable environments (nearby dwarf galaxies not associated with groups or clusters) would provide constraints on the chameleon mechanism that are four orders of magnitude better than current large scale structure limits, and two orders of magnitude better than present solar system tests.

Subject headings: stars: evolution – cosmological parameters – cosmology: theory

1. INTRODUCTION

The discovery of cosmic acceleration a decade ago has spurred a number of attempts to modify general relativity (GR) on large scales. Such attempts generally take the form of a scalar-tensor theory, at least in appropriate limits (e.g. scales small compared to Hubble). The fact that an extra (scalar) force is inevitably introduced is a consequence of a theorem due to Weinberg (1965) and Deser (1970), which states that a Lorentz-invariant theory of a massless spin-two particle must be GR at low energies, or long distances. In other words, to modify the long range interaction between masses, one has no other option but to introduce extra degrees of freedom, such as a scalar field. The force mediated by this scalar must be suppressed or screened in an environment such as the solar system, to satisfy stringent experimental constraints. One common screening mechanism is the chameleon (Khoury & Weltman 2004a,b; Mota & Barrow 2004), where the scalar field has a mass that depends on environment: the mass is large in high density regions (and therefore the scalar force is short range, or Yukawa suppressed), and small in low density ones. The combined scalar + tensor force is thus described by an effective Newton's G that is smaller in screened regions (such as the solar system), and larger in unscreened regions such as voids. As we will discuss below, the precise boundary between screened and unscreened regions or objects is determined by the depth of their gravitational potential.

Several recent papers discuss the observational implications of the chameleon mechanism on structure formation (Oyaizu et al. 2008; Schmidt et al. 2009a), and on equivalence principle violations (Hui, Nicolis & Stubbs 2009; Hui & Nicolis 2010). The latter arises when one compares the motion of a screened versus an unscreened object in an unscreened environment. A screened object does not respond to the scalar field, while an unscreened object does. Therefore, they fall at different rates. Screening affects not only the response of objects to the scalar, but also the sourcing of the scalar field itself. Namely, a screened object does not source the scalar field, while an unscreened object does. This will be important for our discussion below.

In this paper, we show that stellar evolution is modified in such scalar-tensor theories, and in particular the colors and luminosities of red giant branch (RGB) stars are measurably affected. Precision measurement of red giants in distant galaxies would place strong constraints on theories that screen by the chameleon mechanism. The key point is that while a red giant's core is expected to be screened, its envelope could well be unscreened depending on the parameters of the theory. We focus on red giants both because this sort of effect is most pronounced in them, and because they can be observed at great distances. But it should be mentioned that main sequence stars in general will also be affected to some extent by such spatial variations of the effective G. It is also worth mentioning that another screening mechanism, known as the symmetron (Hinterbichler & Khoury 2010), has a lot in common with the chameleon, namely that screened and unscreened objects are distinguished by their gravitational potential. We expect our conclusions on the modification of the red giant's structure to apply to the symmetron case as well. On the other hand, theories that make use of the Vainshtein screening mechanism, such as DGP (Dvali et al. 2000) and the galileon (Nicolis et al. 2009), are not expected to greatly alter red giants' structure, because the screening extent is much less localized than the chameleon or the symmetron.

We begin by giving a brief discussion of the chameleon mechanism in §2, focusing on how it operates inside a star, but also reviewing certain standard results. We

[1] Canadian Institute for Theoretical Astrophysics, 60 St George St, Toronto, ON M5S 3H8, Canada, email: pchang@cita.utoronto.ca
[2] Department of Physics and Institute for Strings, Cosmology and Astroparticle Physics, Columbia University, New York, NY 10027, email: lhui@astro.columbia.edu

then use an appropriately modified version of the stellar evolution code, MESA, (Paxton et al. 2010) to calculate the effects of modified gravity on RGB stars in §3. Finally, we discuss how constraints on these modified gravity theories can be derived from careful measurements of red giants in unscreened galaxies and close in §4.

2. THE SCALAR FIELD

The scalar φ in a chameleon theory is described by

$$\nabla^2\varphi = \frac{\partial V}{\partial \varphi} + \alpha 8\pi G\rho, \tag{1}$$

where V is the self-interaction potential, α is the scalar coupling, and ρ is the mass density. Our notation and normalization follows that of Hui et al. (2009). For instance, $\alpha = 1/\sqrt{2}$ means the (unscreened) scalar force between two masses has exactly the same strength as that mediated by the graviton; $\alpha > 0$ in our convention. We work in Einstein frame.

The potential V is typically chosen such that it is large for small φ and small for large φ, such as in equation (2) below. As a result, the equilibrium value for the scalar field in a high density environment is small, and corresponds to a large mass, which means it is Yukawa suppressed, i.e. screened. Conversely, in a low density environment, the equilibrium value for φ is large, and the scalar field has a small mass and is unscreened. We will use the symbol φ_* to denote the equilibrium value at cosmic mean density ρ_m.

For definiteness, we adopt a potential V of the form:

$$V(\varphi) = B + \frac{A}{\varphi^n}, \tag{2}$$

where B, A and n are constants.[3] Imposing the condition $\varphi = \varphi_*$ for $\rho = \rho_m$ implies:

$$A = 3H_0^2\Omega_m^0\frac{\varphi_*^{n+1}}{n}\alpha, \tag{3}$$

where H_0 is the Hubble constant today, and $\Omega_m^0 = 0.3$ is the matter density today. B should take a value such that $V(\varphi_*)$ accounts for the vacuum energy today:

$$B = 3H_0^2\left[1 - \Omega_m^0(1 + \frac{\alpha\varphi_*}{n})\right]. \tag{4}$$

However, as we are interested in the derivative of V with respect to φ, B is irrelevant for our calculation. As we will see, our conclusions are insensitive to the precise form of the potential, for instance, the choice of n.

For an extended, spherical, object – say a star – described by some mass density field $\rho(r)$, the scalar field profile is determined by equation (1), which can be solved numerically as follows. Discretizing, labeling radial position using the index i, and using the potential outlined above, we can rewrite equation (1) as

$$\frac{\varphi_{i+1} + \varphi_{i-1}}{2} + \frac{\varphi_{i+1} - \varphi_{i-1}}{4}(\Delta \ln r) - \frac{\eta}{2}\rho_i r_i^2$$
$$= \varphi_i - \frac{\eta}{2}\rho_m\left(\frac{\varphi_*}{\varphi_i}\right)^{n+1}r_i^2, \tag{5}$$

[3] Our convention is such that V, and therefore B and A, have dimension of $1/\text{time}^2$, and φ is dimensionless.

where $\eta \equiv \alpha 8\pi G(\Delta \ln r)^2$. Equation (5) with the appropriate boundary conditions ($d\varphi/dr = 0$ for small r and $\varphi = \varphi_*$ for large r) is solved using a nonlinear Gauss-Seidel algorithm with a Newton-Raphson root find at every iteration (Press et al. 1992). More concretely, given a guess for the scalar profile which can be plugged into the left hand side of equation (5), one can solve for φ_i on the right. Iteration then converges to the correct solution.

While this computation gives the most accurate answer for a given $\rho(r)$, it is sufficiently costly that it cannot be used to construct hydrostatic models of stars, which involves repeated calculations of $\rho(r)$ itself. We therefore employ the following ansatz, which is fairly accurate. First, we divide up the star into three regions, a screened center, an unscreened "mantle", and an unscreened exterior. In the screened central region, the scalar field sits at the (small) local equilibrium value at each radius:

$$\frac{dV}{d\varphi} \approx -\alpha 8\pi G\rho. \tag{6}$$

Note that the screened center here might include both the degenerate core of the red giant as well as part of its envelope. In the unscreened "mantle", the scalar field starts to be driven by the density:

$$\nabla^2\varphi \approx \alpha 8\pi G\rho. \tag{7}$$

Finally, outside the star, the density is so much lower that we can approximate

$$\nabla^2\varphi \approx 0. \tag{8}$$

The last approximation remains valid only for r smaller than the Compton wavelength outside the star. In an unscreened environment, this Compton wavelength is much larger than the size of the star, and we assume φ asymptotes to φ_* far away. Essentially the same approximation scheme was worked out in Khoury & Weltman (2004a). The main difference from their solution is that our $\rho(r)$ is not a top-hat, and we have an extended region i.e. the mantle, where the scalar field is unscreened, but the density is non-negligible.

At the radial boundary, $r_{\rm scr}$, between the screened center and the unscreened mantle, let the field value and its derivative be $\varphi_{\rm scr}$ and $k\varphi_{\rm scr}/r_{\rm scr}$, where k is a constant of order unity. By demanding that φ and its derivative are continuous at $r_{\rm scr}$, we find the solution in the unscreened mantle (eq.[7]), $r_{\rm scr} < r < R$ (stellar radius), to be:

$$\varphi(r) = G\int_{r_{\rm scr}}^r dr' \frac{Q(r')}{r'^2} - k\varphi_{\rm scr}\frac{r_{\rm scr}}{r} + (1+k)\varphi_{\rm scr}, \tag{9}$$

where $Q(r) \equiv 8\alpha\pi\int_{r_{\rm scr}}^r \rho(r')r'^2 dr' = 2\alpha[M(r) - M(r_{\rm scr})]$ can be thought of as the scalar charge inside r. Here, $M(r)$ is the mass interior to r. Outside the star $r > R$, the solution to equation (8) is

$$\varphi = \varphi_* - \frac{A}{r}, \tag{10}$$

where A is a constant. Demanding continuity and differentiability at stellar radius R determines A and $r_{\rm scr}$:

$$A \approx GQ(R), \tag{11}$$

$$\frac{GQ(R)}{R} + \int_{r_{\rm scr}}^R \frac{GQ(r)}{r^2} \approx \varphi_*, \tag{12}$$

where we have ignored terms involving $\varphi_{\rm scr} \ll \varphi_*$. The acceleration due to the scalar force is given by $-\alpha\boldsymbol{\nabla}\varphi$. The combined scalar + gravitational radial acceleration $g_{\rm eff}$ is thus

$$g_{\rm eff} = -\frac{G\left(M(r)+\alpha Q(r)\right)}{r^2} \quad \text{for } r > r_{\rm scr}\,,$$

$$g_{\rm eff} = -\frac{GM(r)}{r^2} \quad \text{for } r < r_{\rm scr}\,. \tag{13}$$

The scalar force at $r > r_{\rm scr}$ is sourced only by the unscreened portion of the star, i.e. the scalar charge receives contribution only from the mantle. Within the screened region $r < r_{\rm scr}$, the scalar force is Yukawa suppressed, and therefore the only operating force is gravitational (in the Einstein frame sense). The difference in how the total acceleration relates to $M(r)$, for $r > r_{\rm scr}$ and $r < r_{\rm scr}$, can be interpreted as a spatial variation of an *effective* G. The G used in our expressions throughout is a constant, and corresponds to the value observed in the solar system.

Equations (11) and (12) can be rewritten as

$$\int_{r_{\rm scr}}^{\infty} \frac{GM(r)}{r^2}dr - \frac{GM(r_{\rm scr})}{r_{\rm scr}} \approx \frac{\varphi_*}{2\alpha} \tag{14}$$

The first term is simply (minus) the value of the gravitational potential at $r = r_{\rm scr}$ (fixing the potential to be zero at infinity). The second term is of a similar order. Equation (14) is a more accurate version of the common statement that the gravitational potential defines the boundary between screened and unscreened regions – regions with deeper gravitational potential than $\varphi_*/2\alpha$ are screened ($-$ grav. pot. $\gtrsim \varphi_*/2\alpha$), while regions with shallower potential are not ($-$ grav. pot. $\lesssim \varphi_*/2\alpha$). Note that only two parameters of the chameleon theory are relevant for predicting the scalar force: α which controls the strength, and $\varphi_*/2\alpha$ which controls where screening takes place. Details of the potential V are unimportant.

As a check of the accuracy of our ansatz, in Figure 1, we compare the total force according to our ansatz (eq. [13]) against that from an exact numerical calculation (eq. [5]). We use the same stellar model as in Figure 2 (i.e. same $\rho(r)$). Here, as in elsewhere in this paper unless otherwise stated, we use $\alpha = 1/\sqrt{6}$ which is the value for f(R) (Carroll et al. 2004).[4] Note however this value is not protected by symmetry, the generic expectation is $\alpha \approx O(1)$ (Hui & Nicolis 2010). Figure 1 shows that our ansatz is accurate at the level of $\approx 1\%$. We will use this ansatz to perform our stellar evolution calculation.

3. RED GIANT STRUCTURE IN CHAMELEON GRAVITY

We modified the stellar evolution code MESA (Paxton et al. 2010) to account for the scalar field changes to the local gravity and calculate stellar evolution under these conditions. While the scalar field modified many different aspects of stellar evolution, we focus

[4] Our treatment goes beyond f(R) theories and holds true for any scalar-tensor theory with a scalar interaction of the chameleon (or symmetron) kind. However, it is useful to note the relation between $\varphi_*/2\alpha$ and the analogous parameter in a f(R) theory that arises from a modified action of the type $R \rightarrow R + f(R)$, where R is the Ricci scalar. This relation is: $\varphi_*/(2\alpha) = -(df/dR)/(4\alpha^2) = -1.5(df/dR)$.
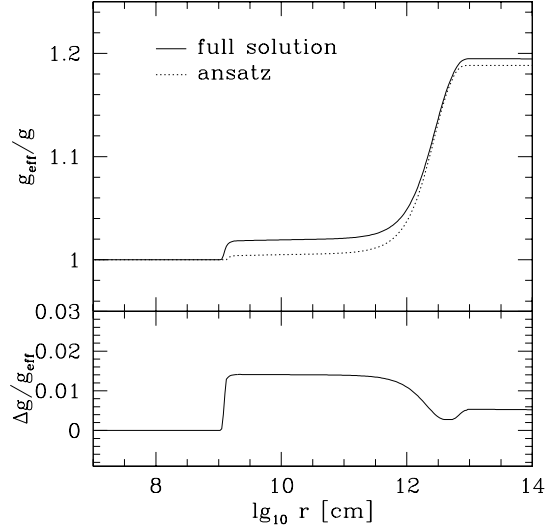

Figure 1. Comparison of the total force (gravitational and scalar) using a full numerical solution and our analytic ansatz, for the density profile of a 1 $M_\odot$ red-giant (Figure 2), and $\varphi_*/2\alpha = 10^{-6}$. The numerical solution uses a potential V (eq. [2]) with $n = 2$. Other choices of n gives very similar results. The upper panel shows the total force, $g_{\rm eff}$, normalized by the gravitational (non-scalar) force, $g = GM(r)/r^2$. The enhancement in the *effective* gravitational force (i.e. total) is $\approx 20\%$ in the outer envelope due to the scalar field (a result of the choice $2\alpha^2 = 1/3$; the enhancement does not reach $1/3$ because of the screened core). The screening radius $r_{\rm scr}$ is located at about 10^9 cm. The lower panel shows the fractional difference in the total force between the numerical and analytic solutions. It is at the percent level.
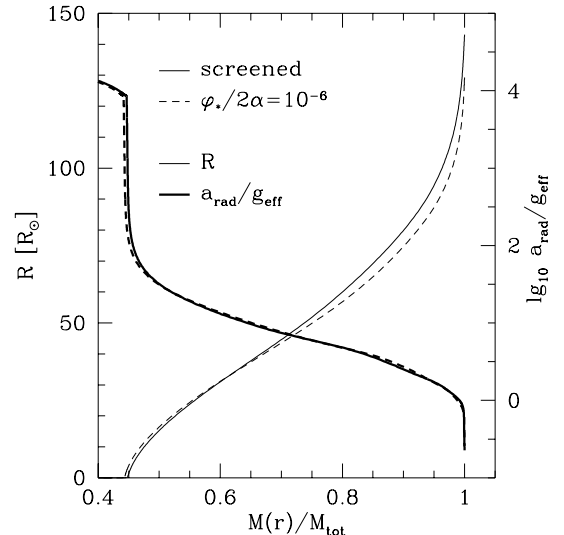

Figure 2. Radius (thin lines) as a function of mass fraction for a 1 $M_\odot$ red giant for a star near the TRGB, with $\varphi_*/2\alpha = 10^{-6}$ (dashed line; core screened) and 0 (solid line; entirely screened i.e. GR), and $2\alpha^2 = 1/3$. Also plotted is the ratio between the radiative acceleration, $a_{\rm rad}$, and effective gravity, $g_{\rm eff}$, in thick lines. The age of the two stars is respectively 10.9 and 11.9 Gyrs for the partially and completely screened case (the age is chosen to yield the same luminosity of 2000 $L_\odot$). Note the 10 $R_\odot$ difference in photospheric radius between these two cases.
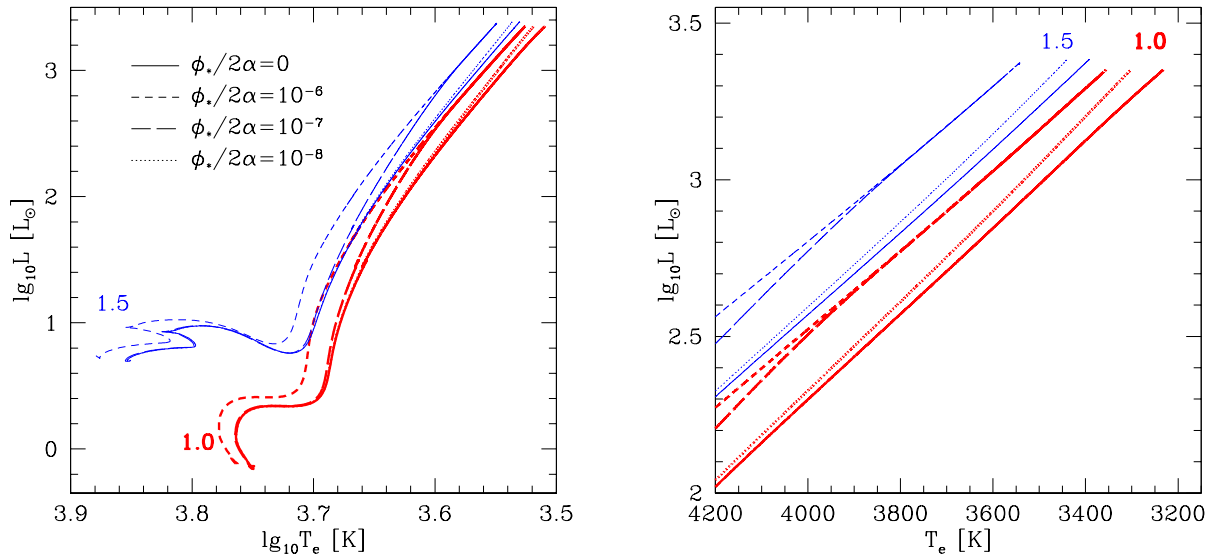
Figure 3. Left plot shows evolutionary track of stars of various masses (denoted in units of solar masses for each track: 1M$_\odot$ in thick red lines and 1.5M$_\odot$ in thin blue lines) for different values of $\varphi_*/2\alpha = 0$ (solid lines; scalar completely screened i.e. GR), 10^{-6} (short-dashed lines), 10^{-7} (long-dashed lines), and 10^{-8} (dotted lines), all with $2\alpha^2 = 1/3$ appropriate for f(R) gravity. Right plot is a closeup of the star on the RGB highlighting the difference between the completely screened star, and the partially screened ones. Note the difference in T_e between the two is ≈ 130 K.

on the RGB phase as these stars are sufficiently bright that they can be observed in distant galaxies (see our discussion in §4). In Figure 2 we show the structure of a $\approx 2\times10^3$ L$_\odot$ RGB star that evolved from a 1 $M_\odot$ main sequence star with $\varphi_*/2\alpha = 10^{-6}$ (i.e. screened at its core) and 0 (i.e. screened in its entirety, meaning GR limit). Solar metallicity is assumed, as in the rest of the paper. The difference in photospheric radius between the two stars is ≈ 10 R$_\odot$ with the completely screened star being larger ($R \approx 145$ R$_\odot$). Because of the smaller radius of the scalar-field influenced star, its effective temperature is larger by ≈ 150 K ($T_{\rm eff} = 3395$ K vs 3258 K).

In Figure 3, we plot the HR diagram for 1 (red) and 1.5 (blue) M$_\odot$ stars with different degrees of screening. We evolve a star from the zero-age main sequence (ZAMS) up to the tip of the red giant branch (TRGB) for $\varphi_*/2\alpha = 0$ (solid lines; no scalar correction i.e. complete screening), 10^{-6} (short-dashed lines), 10^{-7} (long-dashed lines), and 10^{-8} (dotted lines). We have not considered values smaller than $\varphi_*/2\alpha < 10^{-8}$ as the potential depth ($v_{\rm cir}^2/c^2$) of dwarf galaxies are typically $\sim 10^{-8}$. This means that cases where $\varphi_*/2\alpha < 10^{-8}$ are subject to blanket screening: a host galaxy with a potential as shallow as that of a typical dwarf is sufficient to screen the scalar for the star of interest (see §4 for more discussions on blanket screening).

We note the following features. For $\varphi_*/2\alpha = 10^{-6}$, significant departures from the main sequence is immediately apparent, whereas for $\varphi_*/2\alpha = 10^{-7}$ and 10^{-8}, significant deviation do not appear until the RGB phase. That is to say, the scalar field affects the outer envelope for a 1 M$_\odot$ star even on the main sequence, effectively increasing the star's mass (i.e. increasing its photospheric temperature for the same luminosity). This effect is reduced and harder to observe for smaller values of $\varphi_*/2\alpha$. We do not comment on this effect here, choosing instead to focus on RGB stars, but it potentially allows for yet

another probe of modified gravity, albeit for larger values of $\varphi_*/2\alpha$ ($\sim 10^{-6}$). Second, all three $\varphi_*/2\alpha$'s show measurable differences from the the fully screened case (i.e. GR limit) on the RGB. Namely, the scalar-field influenced 1 M$_\odot$ case has nearly the same effective temperature as the 1.5M$_\odot$ RGB for $\varphi_*/2\alpha = 10^{-6}$ and 10^{-7}, i.e., the scalar-influenced star is hotter by ≈ 150 K (this effect is smaller – $\Delta T_{\rm eff} \approx 60$ K – for the $\varphi_*/2\alpha = 10^{-8}$ case).

To develop a better qualitative understanding of why red giants are such good probes of chameleon gravity, we plot the ratio of the radiative acceleration, $a_{\rm rad}$, and the effective gravity, $g_{\rm eff}$ (total scalar + gravitational acceleration), as a function of mass fraction in Figure 2. Here we define $a_{\rm rad} = \kappa L/4\pi r^2 c$ as a function of the *total* luminosity, L, where κ is the Rosseland mean opacity. As $a_{\rm rad} > g_{\rm eff}$ for the vast majority of the envelope, the energy flux is not carried outward by radiation, but rather by convection (Kippenhahn & Weigert 1990; Paczyński 1969). Only near the photosphere, where $a_{\rm rad} = g_{\rm eff}$, can radiation carry away the star's luminosity. It is this condition $a_{\rm rad} = g_{\rm eff}$ that determines the position of the photosphere for both the fulled screened and partially screened (scalar-influenced) star.

The opacity in the envelope is dominated by H$^-$ opacity, which scales like T^9 for $3000 \lesssim T \lesssim 6000$ K (Hansen et al. 2004). The scaling between effective gravity of the red giants (due to scalar fields) and the photospheric temperature of $\epsilon_{\rm eff} \sim 9\Delta T_{\rm ph}/T_{\rm ph}$ then gives

$$\Delta T_{\rm ph} \approx 110 \left(\frac{T_{\rm ph}}{4000\,{\rm K}} \right) \left(\frac{\epsilon_{\rm eff}}{0.25} \right) \,{\rm K}, \qquad (15)$$

which roughly matches what we are finding in the full calculation.

Finally in Figure 4, we consider the effect of different values of the scalar coupling, α, on RGB structure for three different values of $\varphi_*/2\alpha = 10^{-6}$, 10^{-7} and
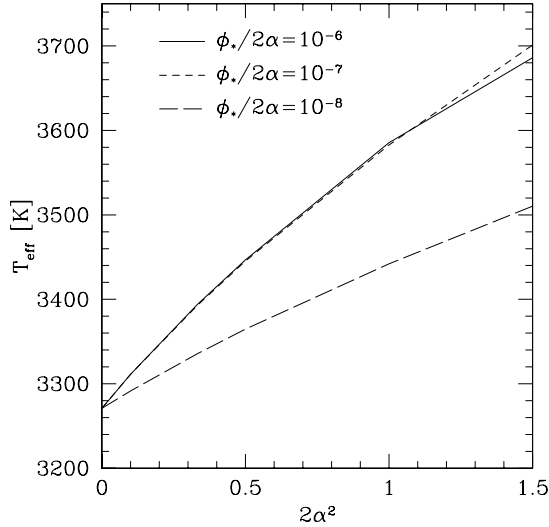
Figure 4. The effective temperature as a function of the scalar coupling, $2\alpha^2$, for a $L = 2000L_\odot$, $1M_\odot$ RGB star. For a red giant that is not under the influence of a scalar field, i.e., $2\alpha^2 = 0$, $T_{\rm eff} \approx 3270\,{\rm K}$. As the coupling of the scalar field increases, $T_{\rm eff}$ increases, a result of the smaller size of the RGB star.

10^{-8}. We plot the effective temperature of a $2000L_\odot$ RGB star for different values of the scalar coupling. The case of no scalar coupling $2\alpha^2 = 0$ is the GR limit, where $T_{\rm eff} \approx 3270$ K. As α increases, the effective temperature increases. For instance the effective temperature is ≈ 3400 K for $2\alpha^2 = 1/3$ (the f(R) gravity case we studied above), which is an increase of ≈ 130 K over the unmodified case. For $2\alpha^2 = 1.5$, $T_{\rm eff} \approx 3700$ K, an increase of over 400 K above the fully screened case.

4. DISCUSSION

As we have mentioned, we have mainly focused on RGB stars as they are observable in distant galaxies due to their large luminosity. Indeed tip of the RGB stars are seen out to ≈ 30 Mpc (Mager et al. 2008) and used for accurate distance measurements (see the review Freedman & Madore 2010). We have shown above that their temperature is also very susceptible to the effects of scalar fields. We now discuss their use as constraints on modified gravity theories.

First let us discuss the precision with which their temperature can be measured. Ferraro et al. (2006) (see also Cassisi 2007) collected high quality J, H, and K photometry of 28 Galactic globular clusters to measure the effective temperatures of RGB stars at fixed bolometric luminosities. Their measurement uncertainty of $\approx \pm 30 - 60$ K suggests that measuring an effective temperature difference of ≈ 150 K is quite viable. For a scalar-matter coupling α larger than $1/\sqrt{6}$, the expected temperature difference should be even larger.

We caution other effects are also important in influencing the temperature of RGB stars. For instance, metallicity can change the effective temperature of a RGB star by a few hundred K (see Figure 4 of Cassisi 2007 or Figure 2 and 3 of Ferraro et al. 2006). Fortunately, metallicity effects are well modeled using modern stellar evolution codes (again see Figure 4 of Cassisi 2007). A constraint on the metallicity of these stars, e.g., spectroscopic measurements, will help mitigate these effects. There are also

additional effects that might contribute, i.e., uncertainties in mixing-length theory, conductive opacities, etc, but these are being mitigated via comparison to local RGB stars.

The effects of modified gravity on stellar evolution (for $\phi_*/2\alpha \sim 10^{-8} - 10^{-7}$) would also manifest itself in deviation of the RGB branch under modified gravity (see Figure 3). This deviation would be a unique signature of modified gravity compared to metallicity variations. Constraining this deviation in "clean" system such as globular clusters around unscreened galaxies would also place limits on the parameter of the chameleon mechanism.

As is apparent from Figure 3, the mass of the initial star may also shift the color of these TRGB stars so that they appear bluer. Namely the degeneracy between scalar field effects and mass of the RGB star needs to be broken. An examination of Figure 3 suggests several methods by which this can be done. If $\varphi_*/2\alpha$ is small, the deviation from the RGB track due to the effect of the scalar field can be used to directly test for the strength of the scalar field. However, for a sufficiently large $\varphi_*/2\alpha$, this happens sufficiently early in the RGB phase that the deviation might be missed. In that case, the mass of these RGB stars would need to be established and this can happen in several ways. For instance, if the stellar population is relatively uniform and a clean turnoff mass can be identified, this would put a strong constraint on the mass of the progenitor. Note that the RGB track for the scalar influenced 1 $M_\odot$ traces the (fully) screened 1.5 $M_\odot$ track fairly closely. However, the positions of the turnoff for 1 and 1.5 $M_\odot$ stars are significantly different.

We now discuss the current constraints on chameleon theories, and examine what kind of host galaxies are needed to improve them. Stringent tests of GR in the solar system tell us that the scalar must be screened within it. The simplest interpretation is that the solar system is screened by virtue of its residing inside the Milky Way (MW), which has a self gravitational potential of $\sim -10^{-6}$. [5] This suggests $\varphi_*/2\alpha \lesssim 10^{-6}$ so that the MW, and therefore its constituent solar system, is screened. [6] This could possibly be evaded by saying that the MW is screened not so much by its self gravitational potential, but by virtue of its residing in the local group. But data and constrained realizations suggest the local group has a gravitational potential rather similar to that of the MW itself (Klypin et al. 2003). Neighbors of the local group are unlikely to change the picture significantly – for instance, both the Virgo cluster and the local void contributes a potential at the MW of the order of 10^{-6}, with opposite signs (Peebles & Nusser 2010). Structure formation offers a constraint independent of such MW considerations: $\varphi_*/2\alpha \lesssim 10^{-4}$ from the observed cluster abundance (Schmidt et al. 2009b). We

---

[5] By coincidence, the sun has a similar gravitational potential, $\sim -2 \times 10^{-6}$.

[6] Another option is of course that the scalar-matter coupling α is very close to zero. This is the uninteresting limit of the scalar force being practically invisible to everything else. Our discussion assumes instead gravitational strength coupling of $\alpha \sim O(1)$, including for instance the f(R) value of $\alpha = 1/\sqrt{6}$. Observational constraints on chameleon theories ultimately translate into limits on the plane of $\varphi_*/2\alpha$ and α (see Fig. 3 of Hui et al. 2009).

will frame our discussion mainly in terms of improving the MW constraint of 10^{-6}, though obviously the improvement will be even greater when compared against the more conservative structure formation limit.[7]

Red giants located in a host galaxy with a gravitational potential shallower than the MW can improve upon the existing constraint. For instance, a 100 km/s host galaxy could push the limit on $\varphi_*/2\alpha$ to 10^{-7}; a 30 km/s dwarf could push it to 10^{-8}. The important point is to avoid blanket screening, i.e. avoid host galaxies that are screened by their surroundings, such as by virtue of being situated inside a cluster or massive group.[8] This means that for red giants located within a 100 km/s galaxy to be useful, we would like to make sure the galaxy's surroundings contribute a potential no deeper than -10^{-7}. This should be achievable if the galaxy is located at a distance of more than a few Mpc from the MW[9], avoiding the local sheet and into the general direction of the local void (Klypin et al. 2003). For red giants located within a 30 km/s dwarf to be useful, we should make sure the galaxy's neighbors contribute a potential no deeper than -10^{-8}. For this, one could venture deeper into the local void (Peebles & Nusser 2010) , or go to the field or voids that are further away from nearby concentrations of galaxies ($\gtrsim$ 10 Mpc, Szomoru et al. 1996a,b; Rojas et al. 2004; van de Weygaert et al. 2009; Stanonik et al. 2009). Obviously, an accurate mapping of the gravitational potential of the local universe ($\lesssim$ tens of Mpc) would be highly desirable in determining which galaxies are likely to be unscreened by environment.

In this paper, we have shown that RGB stars in galaxies with shallower potential than the MW can be used to improve constraints on modified gravity theories that invoke the chameleon or symmetron mechanism. We have shown that RGB stars with an unscreened envelope (but generally screened core) are more compact, and hence hotter (by $\approx$ 150 K) than completely screened RGB stars (like the ones in the MW) at the same luminosity. This temperature difference should be measurable in distant unscreened galaxies. Dwarf galaxies in the field or in voids will give us the strongest limits, improving the current solar system or MW constraint by 2 orders of magnitude, and current structure formation constraints by 4 orders of magnitude.

REFERENCES

Adams, F. C. 2008, J. Cosmology Astropart. Phys., 8, 10

Carroll, S. M., Duvvuri, V., Trodden, M., & Turner, M. S. 2004, Phys. Rev., D70, 043528

Cassisi, S. 2007, in IAU Symposium, Vol. 241, IAU Symposium, ed. A. Vazdekis & R. F. Peletier, 3–12

Deser, S. 1970, Annals Phys., 59, 248

Dvali, G. R., Gabadadze, G., & Porrati, M. 2000, Phys. Lett., B485, 208

Ferraro, F. R., Valenti, E., Straniero, O., & Origlia, L. 2006, ApJ, 642, 225

Freedman, W. L., & Madore, B. F. 2010, ArXiv e-prints

Hansen, C. J., Kawaler, S. D., & Trimble, V. 2004, Stellar interiors : physical principles, structure, and evolution, ed. Hansen, C. J., Kawaler, S. D., & Trimble, V.

Hinterbichler, K., & Khoury, J. 2010, Phys. Rev. Lett., 104, 231301

Hui, L., & Nicolis, A. 2010, Phys. Rev. Lett., in press, [arXiv:1009.2520 [hep

Hui, L., Nicolis, A., & Stubbs, C. W. 2009, Phys. Rev. D, 80, 104002

Khoury, J., & Weltman, A. 2004a, Phys. Rev., D69, 044026

—. 2004b, Phys. Rev. Lett., 93, 171104

Kippenhahn, R., & Weigert, A. 1990, Stellar Structure and Evolution, ed. Kippenhahn, R. & Weigert, A.

Klypin, A., Hoffman, Y., Kravtsov, A., & Gottloeber, S. 2003, Astrophys. J., 596, 19

Mager, V. A., Madore, B. F., & Freedman, W. L. 2008, ApJ, 689, 721

Mota, D. F., & Barrow, J. D. 2004, Mon. Not. Roy. Astron. Soc., 349, 291

Navarro, J. F., Frenk, C. S., & White, S. D. M. 1996, ApJ, 462, 563

Nicolis, A., Rattazzi, R., & Trincherini, E. 2009, Phys. Rev., D79, 064036

Oyaizu, H., Lima, M., & Hu, W. 2008, Phys. Rev., D78, 123524

Paczyński, B. 1969, Acta Astronomica, 19, 1

Paxton, B., Bildsten, L., Dotter, A., Herwig, F., Lesaffre, P., & Timmes, F. 2010

Peebles, P. J. E., & Nusser, A. 2010, Nature, 465, 565

Press, W. H., Teukolsky, S. A., Vetterling, W. T., & Flannery, B. P. 1992, Numerical recipes in FORTRAN. The art of scientific computing, ed. Press, W. H., Teukolsky, S. A., Vetterling, W. T., & Flannery, B. P.

Rojas, R. R., Vogeley, M. S., Hoyle, F., & Brinkmann, J. 2004, ApJ, 617, 50

Schmidt, F., Lima, M. V., Oyaizu, H., & Hu, W. 2009a, Phys. Rev., D79, 083518

Schmidt, F., Vikhlinin, A., & Hu, W. 2009b, Phys. Rev., D80, 083505

Stanonik, K., et al. 2009

Szomoru, A., van Gorkom, J. H., & Gregg, M. D. 1996a, AJ, 111, 2141

Szomoru, A., van Gorkom, J. H., Gregg, M. D., & Strauss, M. A. 1996b, AJ, 111, 2150

van de Weygaert, R., et al. 2009

Weinberg, S. 1965, Phys. Rev., 138, B988

---

[7] Indeed, if $\varphi_*/2\alpha$ were larger than about 4×10^{-5}, even the red giant core would start to be unscreened (assuming its host galaxy is unscreened), and the predicted modifications to the luminosity-temperature relationship would be greater. A discussion of the behavior of stars under strongly modified physical constants (including G) is found in Adams (2008).

[8] In other words, screening communicates from host to members. A red giant inside a galaxy inside a cluster is screened because of the deep potential of the cluster, even if the galaxy does not have a deep *self*-potential.

[9] Our calculations of the screening effect in an NFW profile (Navarro et al. 1996) suggest that the blanket screening of the MW halo is important up to a few times r_{200}, so that the local dwarfs are likely not useful for this measurement.